Time Domain Electromagnetic Simulation for Microwave CAD Applications

Wolfgang J. R. Hoefer, *Fellow, IEEE*

***Abstract*—Rapid progress in time domain modeling and computer technology have brought practical time domain simulators within reach. The next decade will see the emergence of sophisticated time domain simulation tools linking geometry, layout, physical and processing parameters of a microwave or high speed digital circuit with its system specifications and the desired time and frequency performance, including electromagnetic susceptibility and emissions. These CAD systems will most likely employ dedicated parallel processors configured specifically for modeling three-dimensional field problems. Furthermore, the nature of discrete time domain algorithms allows the designer to employ optimization and synthesis procedures which differ from those employed in traditional frequency domain CAD tools. In this paper, recent progress in time domain modeling will be highlighted, and the possible impact of these development on future CAD procedures and systems will be discussed.**

I. Introduction

Computer aided design (CAD) of microwave circuits, including nonlinear analysis, is almost exclusively performed in the frequency domain. The principal reason lies in the historical development of electromagnetic field analysis in communication and broadcasting engineering. Time domain analysis was, at least in the first half of the twentieth century, mostly performed in high voltage engineering in order to deal with transients due to switching, loading changes, breakdown and lightning. Later, the development of digital techniques for communications, measurement (time domain reflectometry) and high speed logic have generated greater interest in time domain analysis, both at the circuit and the field levels.

In order to reduce the computational complexity of a field problem it is, of course, both reasonable and desirable to reduce the number of independent variables by using Fourier transform techniques. In this way, the time dimension can be eliminated by assuming sinusoidal time dependence. Furthermore, if a structure is uniform in one or even two space dimensions, the problem can be broken down into simpler steady-state periodic solutions. The spectral domain approach is a good example of this procedure. In more general terms, traditional field analysis transforms the physical situation into a mathematical model by projecting or mapping the space-time problem into one or several abstract domains where the solution procedure is simplified. This traditional approach to field analysis is summarized in Fig. 1(a). The important point here is that the formulation of the problem includes the specific boundary topology and material composition, as reflected, for example, by the choice of basis functions in a spectral domain solution, or the choice of eigenmodes in a mode-matching solution. Typical examples are spectral domain programs for multi-layer planar circuit structures, or mode-matching programs for waveguide filters. This extensive analytical pre-processing leads to computationally efficient algorithms which, when implemented on powerful computers, result in efficient field solving tools.

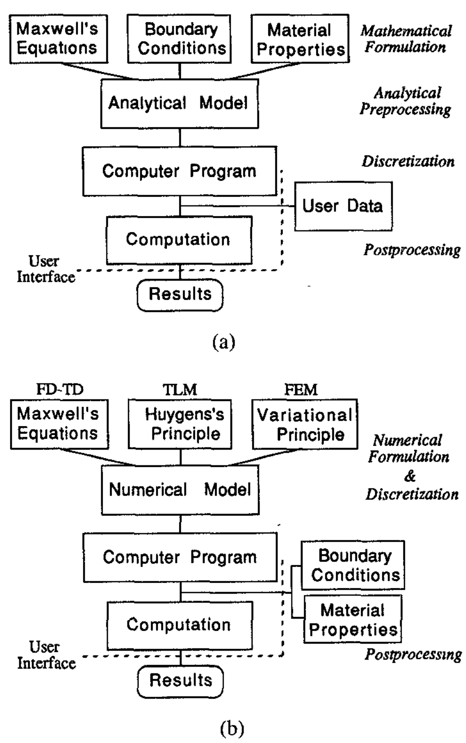

Fig. 1. Traditional (a) and alternative (b) approach to electromagnetic modeling of microwave structures.

Naturally, these tools are well suited for specific types of circuit topologies associated with well defined manufacturing technologies. However, the user of such tools can only control the geometrical and electrical parameters

Manuscript received September 4, 1991; revised February 17, 1992.

The author is with the Department of Electrical and Computer Engineering, University of Victoria, P.O. Box 1700, Victoria, BC, Canada V8W 2Y2.

IEEE Log Number 9108315.

of the structure under study, but not its essential configuration. It is also very difficult to obtain with such methods the response of a circuit to arbitrary waveform excitation, particularly in the presence of dispersion and nonlinearities. However, this is usually acceptable in return for computational efficiency, provided that the circuit technology is well defined.

In recent years, however, alternative approaches have emerged which provide greater flexibility to the user at the expense of larger computational requirements. (Fig. 1(b)). Here, the principal algorithm models the intrinsic behavior of electromagnetic fields without reference to specific boundary and material configurations; it can be formulated either for time-harmonic or general time-dependent fields in three-dimensional space, thus forming the basis for a frequency domain or a time domain electromagnetic simulator, respectively. It is up to the user to specify every detail of the structure to be modeled. While it demands a considerable user input, such an approach extremely general and flexible; it allows the user to tackle previously unsolved structures without the need for special expertise in field theory, mathematics and numerical techniques. This does, of course, not imply that circuit designers need to be less knowledgeable when using such a tool, but rather that the tools available to circuit designers become more powerful and versatile. As the available computing power increases, the larger CPU time and memory requirements compared to that of a specialized code based on extensive analytical pre-processing, becomes less relevant within the overall context of electromagnetic design. One could almost speak of a paradigmatic shift in electromagnetic field modeling. Among the factors that are driving this evolution, the following are the most obvious:

a) The rapid increase in speed and memory of digital computers, as well as the availability of vector computers and parallel processors.
b) The increasing complexity, density and operating frequency of electromagnetic structures, as well as the need to study their response to non-sinusoidal waveforms. Typical examples include monolithic integrated microwave circuits, high speed digital electronics, and EMI/EMC problems.
c) The requirements of potential users of numerical field modeling tools. The most important are the ability to solve realistic problems of arbitrary geometry, reliability, accuracy and numerical stability, time and frequency domain capability, user friendliness, extraction of relevant parameters, compatibility with already existing CAD tools, and the possibility of field visualization and animation.

One of the principal virtues of powerful processors is that they make it possible to model electromagnetic processes directly in space and time, the natural dimensions in which dynamic physical events are experienced. For maximum efficiency of digital processing, problems are formulated directly in numerical, algorithmic rather than in analytical form, and executed following a time-stepping procedure. This has the advantage that boundary conditions, electrical composition and excitation of a structure which are characteristic of a particular problem, do not restrict the basic algorithm, but are input by the user, preferably through a graphics interface (See Fig. 1(b)).

The evolution of microwave CAD closely follows that of electromagnetic analysis while depending strongly on available computer performance. Thus, earlier tools for microwave design were based on equivalent circuit representation and closed-form expressions, but modern versions employ increasingly some form of frequency domain field analysis and computer-generated multidimensional lookup tables. Design is performed by repeated analysis combined with appropriate optimization strategies.

Another important development is the combination of electromagnetic modeling with interactive computer graphics. Through field visualization and animation, electromagnetic field behavior can be observed directly, enabling the designer to relate the properties of a circuit to the behaviour of the fields and thus give physical meaning to abstract formalism.

However, modeling electromagnetic fields in the time domain requires a number of new concepts and procedures which, when implemented efficiently in the form of a time domain electromagnetic simulator, are opening new horizons in microwave CAD. In this paper, important developments in time domain field modeling will be highlighted, and their practical implementation in the form of CAD tools for process-oriented microwave circuit design will be demonstrated. Finally, future development trends will be discussed.

II. Basic Properties of Time Domain Simulators

A. Time-Stepping Algorithms

Discrete time domain models of electromagnetic fields can be obtained by discretizing time domain differential or integral formulations, by discrete spatial network representation of fields, or by finite element approximation. The large majority of time-domain simulators, however, is based either on a discretization of Maxwell's equations in differential form (Finite Difference—Time Domain, or FD-TD method) or on a discrete spatial network model (Transmission Line Matrix, or TLM method).

While FD-TD is formulated in terms of electric and magnetic field components, TLM exploits the analogy between field propagation in space and voltage/current propagation in a spatial transmission line network, which is formulated as a multiple scattering process following Huygens' principle. As a general rule, both methods lead to practically identical results; in fact, for each TLM scheme there exists an equivalent FD-TD formulation, and *vice versa*, which means that one can be derived from the

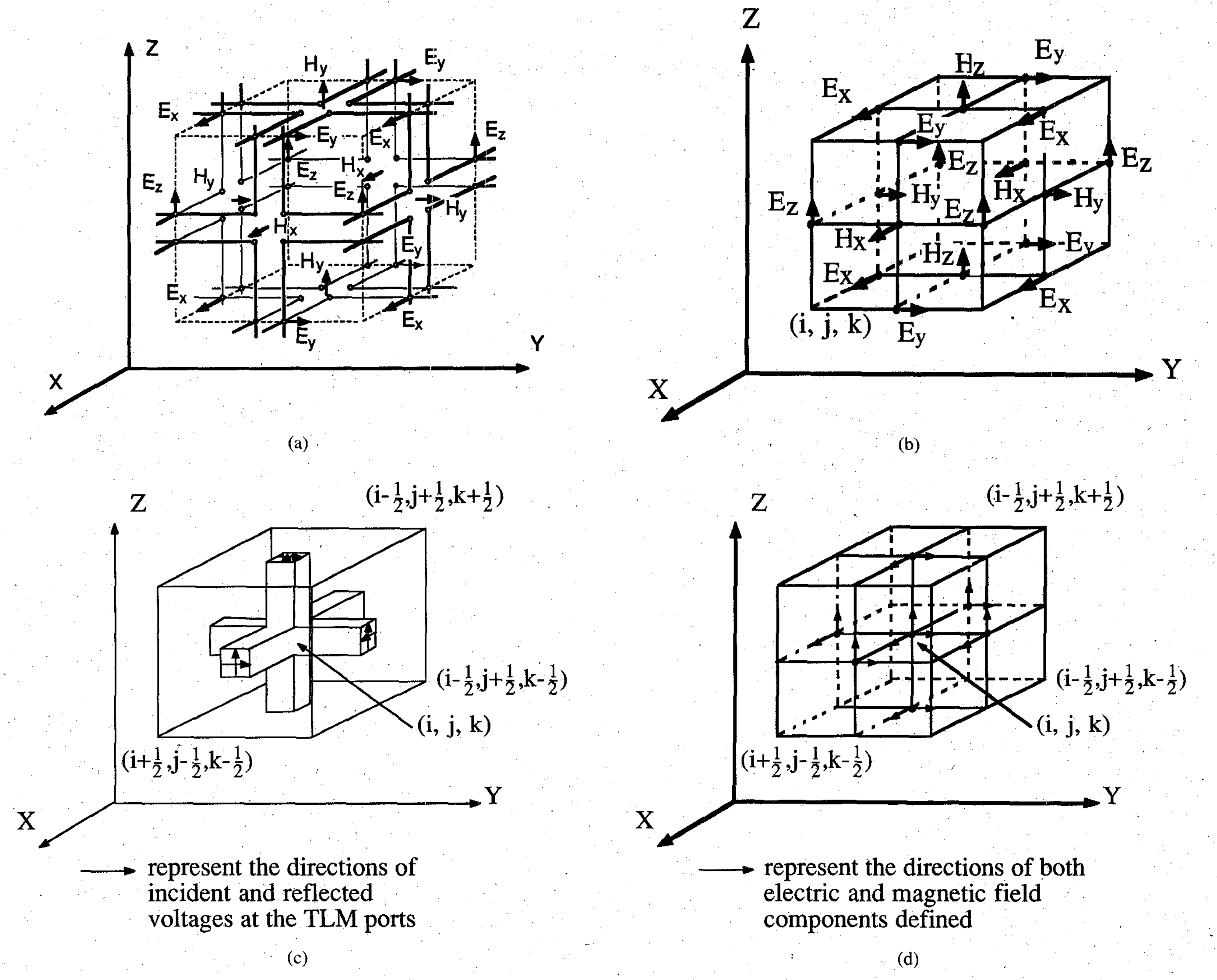

Fig. 2. Various schemes for time-space discretization of electromagnetic field problems. (a) Johns' distributed 3-D TLM node [1]; (b) Yee's Finite Difference—Time Domain grid [2]; (c) Johns' condensed 3-D TLM node [3]; (d) FD-TD grid proposed by Chen *et al.* [4].

other. Fig. 2 shows two such pairs of equivalent schemes. Fig. 2(a) and (b) show Johns' distributed TLM node [1] and Yee's unit FD-TD cell [2]. Fig. 2(c) and (d) compare Johns' condensed TLM node [3] and the equivalent FD-TD scheme derived by Chen *et al.* [4]. One basis for comparing discrete time domain field models is their dispersion of the propagation vector. It is well known that the dispersion in a discrete system is equal to that in its generic continuous system only in the infinitesimal limit of the discretization step ($(\Delta l/\lambda) \rightarrow 0$), and it deviates from it the more $\Delta l/\lambda$ increases. Fig. 3 shows the dispersion characteristics of the discretization schemes in Fig. 2 as derived by Nielsen and Hoefer [5]. These dispersion surfaces are the loci for the propagation vector in the three-dimensional discretized propagation space. For low frequencies ($(\Delta l/\lambda << 1$) the dispersion surfaces form a unit sphere in all cases, which means that propagation is isotropic and nondispersive. However, at higher frequencies, the dispersion of the condensed TLM node and Chen's FD-TD scheme is considerably smaller than that of the other two schemes in Fig. 2(a) and (b).

Clearly, equivalent TLM and FD-TD schemes possess identical dispersion characteristics. Furthermore, optimized codes for equivalent schemes require a similar computer memory and execution time. Nevertheless, they have their respective advantages and disadvantages when implementing boundaries, dispersive constitutive parameters, and nonlinear devices. In the final analysis, the choice between TLM or FD-TD is mostly based more on personal preferences and familiarity with one or the other method. In the following, the salient features of time domain simulators will thus be described in terms of TLM formalism with the understanding that there exists, or can be derived, an equivalent FD-TD formulation.

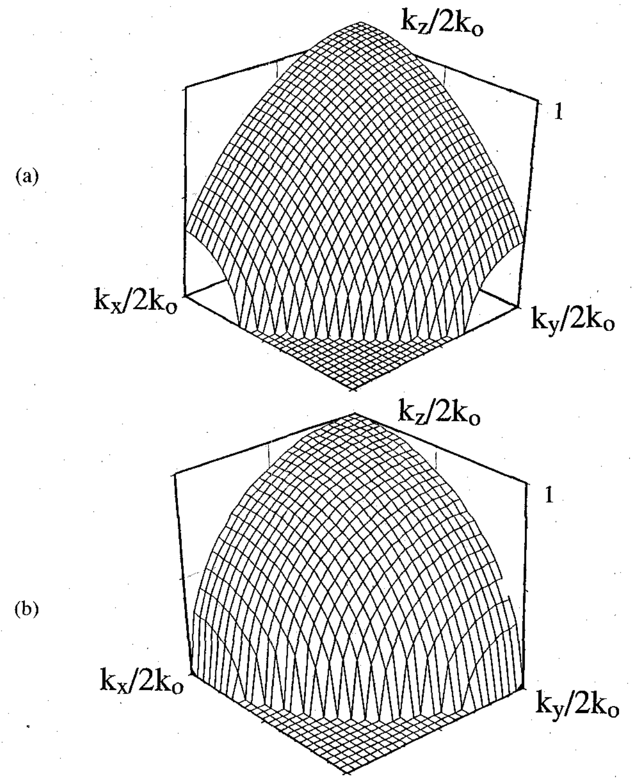

Fig. 3. Plots of the dispersion surfaces for the schemes shown in Fig. 2(a) Expanded TLM node and Yee's FD-TD scheme; (b) Condensed TLM node and Chen's FD-TD scheme. (Normalized frequency $2\pi\Delta l/\lambda = 0.7$. Stability factor for the FD-TD schemes $s = 0.5$. The surfaces are perfect unit spheres when $2\pi\Delta l/\lambda = 0$).

B. Advantages of Time Domain Analysis

The principal advantages of modeling electromagnetic fields in the time domain are the following:

1) Non-sinusoidal waveforms and transient phenomena can be studied directly.
2) Nonlinear and frequency dispersive behaviour can be modeled more physically in the time domain than in the frequency domain where the representation of these properties is mostly phenomenological.
3) Properties over a wide frequency band can be obtained with a single impulsive analysis.
4) The geometry and the electromagnetic material properties of a structure can be varied during a simulation through modeling of moving boundaries and time varying constitutive parameters.
5) Direct numerical synthesis is possible through reversal of electromagnetic processes in time.
6) Due to the localized character of time domain algorithms, they are particularly well suited for implementation on parallel or vector processors.

However, in order to implement these capabilities in a practical simulator, dispersive and nonlinear properties, moving boundaries, and sophisticated signal processing procedures must be implemented, which include forward and inverse Fourier transforms, numerical convolution, and wideband absorbing boundaries. The latter are required for the extraction of scattering parameters from the impulse response of dispersive guiding structures, and for the truncation of the computational domain when modeling free-space scattering and radiation problems. Another important requirement is a graphic user interface for 3-D geometry editing, parameter extraction and display, as well as dynamic visualization of fields, charges and currents. Last, but not least, compatibility with existing CAD tools is important, requiring the transfer of simulation data in the appropriate formats.

The feasibility of these features has been demonstrated both in TLM and FD-TD environments [6]–[8]. However, the computational requirements for modeling complex structures with such methods are still extremely severe. Therefore, research efforts are being focused on the development of techniques to improve computational efficiency, the most important of which will be discussed next.

III. Techniques for Improving Computational Efficiency

One of the main objectives in time domain modeling research is the reduction of computational expenditure. In the following, the most important techniques for achieving this objective will be briefly described. The first exploits the localised nature of the time domain algorithms through parallel processing, the second is based on the numerical processing of the time domain output signal using Prony's Method, and the third involves the reduction of the so-called coarseness error due to insufficient resolution of highly nonuniform fields by the finite discretization in the vicinity of sharp corners and edges. Even though these techniques will be described below for TLM modeling, they can be implemented in FD-TD schemes as well.

A. Parallel Processing

The principle of causality ensures that any local change in the discretized field space affects only its immediate neighbourhood at the next computational step. The highly localised nature of time domain algorithms is therefore perfectly suited for parallel processing. The type of machine most suitable for the implementation of such algorithms is the SIMD system (Single Instruction Multiple Data) such as the "Connection Machine" of Thinking Machines Inc., which consists of a large number of processors (up to 16 384) that are networked together. The processors have their own memory banks and operate on instructions broadcast to them by a host computer.

This allows implementation in a form quite different from the program on a serial machine. Since each processor has its own memory, it is practical to assign, in the TLM case, to each of them in an impulse scattering matrix and a set of boundary conditions. The impulse scattering matrix incorporates the local properties of the computational space such as permittivity, permeability, conductivity, and mesh size in the three co-ordinate directions. The boundary conditions specify whether there are boundaries between a node and its neighbours, or whether the nodes are connected together. This parallel implementation greatly facilitates variable mesh grading, conformal boundary modeling, and the simulation of highly inhomogeneous materials and complicated geometries.

In order to assess the impact of parallel processing on the computing speed we have implemented the 3-D TLM condensed node on the Connection Machine of the INRIA Computing Centre at Sophia Antipolis, France. The gain in performance is impressive. Fig. 4 compares, on a logarithmic scale, the improvements made over the last year in computing speed using various programming techniques [9] and parallelisation. The original matrix formulation by Johns [3] requires 144 multiplications and 126 additions/subtractions per scattering per node. Through manipulation of the highly symmetrical impulse scattering matrix, Tong and Fujino [9] have reduced the scattering to six multiplications, 66 additions/subtractions and 12 divisions by four, increasing computing speed over six times. Programming in Assembler rather than C++ accelerates the process again four times. Finally, parallel processing increases speed by more than two orders of magnitude over the fastest serial version implemented on a 386 computer in C++ language. The combined measures effectively reduce computation times from hours to seconds.

This comparison strongly suggests that future implementations of time domain simulators for CAD purposes will be based on dedicated parallel processors or supercomputers that emulate parallel processing.

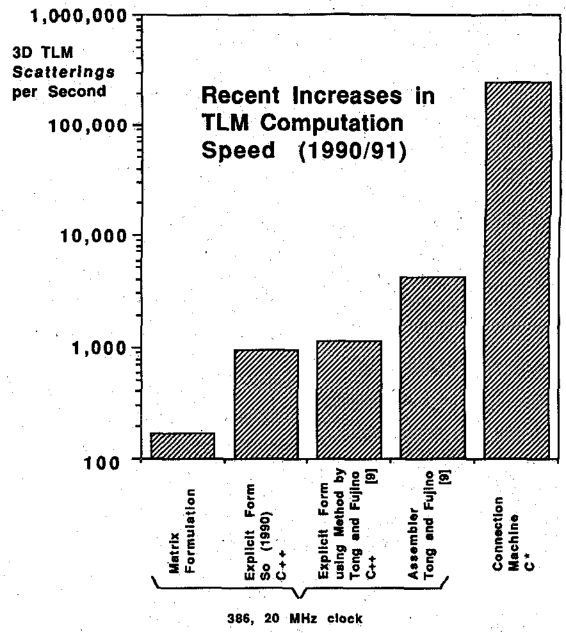

Fig. 4. Recent increases in the speed of TLM computations.

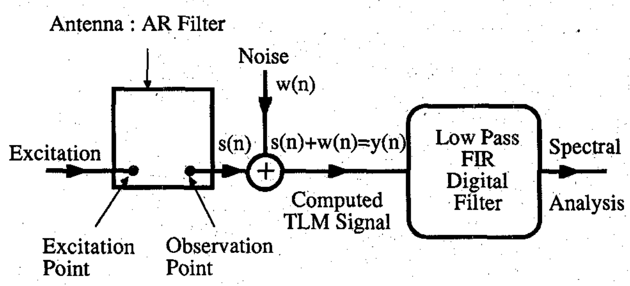

Fig. 5. Model of the Prony–Pisarenko method for TLM signal processing (after Dubard *et al.* [10]).

B. Signal Processing

The fast Fourier Transform (FFT) is the most frequently used signal processing method for extracting the spectral characteristics of a structure from a time domain simulation. For a realistic structure such as a planar antenna, typically 60 000 iterations (time samples) at 3,000 space points requiring 23 Mbytes of memory storage are needed to get the radiation pattern, but even this is insufficient for computing the input impedance of the antenna. It is therefore of prime importance to reduce the number of time samples required to extract a meaningful frequency response. To achieve this goal, processing of the time response using Prony's method has been applied successfully [10], [11].

In this approach the discrete time domain output signal is treated as a deterministic signal drowned in noise. (Fig. 5). The signal is then approximated by a superposition of damped exponential functions (Prony's method), and the noise is minimized using Pisarenko's model. This signal processing technique reduces the number of required time samples by typically one order of magnitude.

C. Reduction of Coarseness Error

One of the principal sources of error in the TLM analysis of structures with sharp edges and corners is the so-called coarseness error. It is due to the insufficient resolution of the edge field by the discrete TLM network. The error is particularly severe when boundaries and their corners are placed halfway between nodes as shown in Fig. 6. It is clearly seen that the nodes situated diagonally in front of an edge are not interacting directly with the boundary but receive information about its presence only across their neighbours who have one branch connected to it. The network is thus not sufficiently "stiff" at the edge, i.e., the edge field is not sufficiently coupled to the edge current, and results obtained in these cases are always shifted towards lower frequencies. The classical remedy for this problem is to use a finer mesh in the vicinity of the edge, but this introduces additional complications and computational requirements. On the other hand, the dispersion characteristics of the condensed 3-D TLM node (see Fig. 3(b)) are so good that the velocity error is practically negligible even for rather coarse meshes. A much better and more efficient way is thus to modify the corner node such that it can interact directly with the boundary corner through an additional stub as shown in Fig. 7 for the 2-D case [12]. Since this stub is longer than the other branches by a factor $\sqrt{2}$ it is simply assumed to have a correspondingly larger propagation ve-

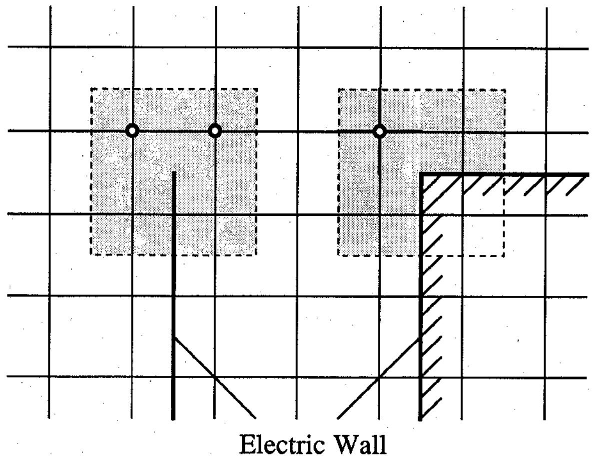

Fig. 6. Corner nodes in 2-D TLM mesh are not interacting directly with the boundaries, causing large coarseness error.

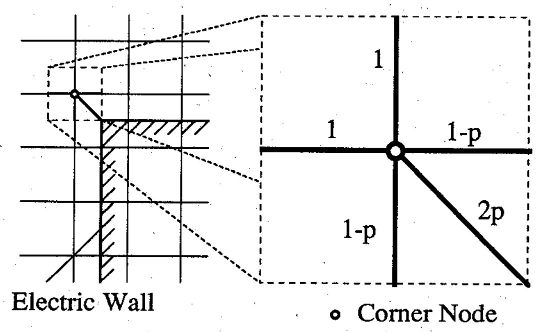

Fig. 7. Compensation of coarseness error by adding a fifth branch to the corner node.

locity. The effect of this corner correction is demonstrated in Fig. 8 which shows typical results for the first resonant frequency of a cavity containing a sharp edge as a function of the mesh parameter Δl (see [12]). The parameter p is proportional to the fraction of power carried by the fifth branch of the corner node and is equal to half the characteristic admittance of the corner branch when normalized to the link line admittance (see Fig. 7). For $p = 0$ (no corner correction) the coarseness error increases almost linearly with increasing Δl, while for $p = 0.1$ the frequency remains accurate even for a very coarse mesh. The simplest and most accurate method for finding this optimum value of p is to determine it empirically in such a way that the resonant frequency becomes independent of the mesh size as demonstrated in Fig. 8. Numerous numerical experiments using different geometries and frequencies have confirmed that the optimal $p-$ value is insensitive to these factors. For more detail the reader is referred to [12].

IV. Arbitrary Positioning of Boundaries

A. Accurate Dimensioning and Curved Boundaries

The accurate modeling of waveguide components, discontinuities and junctions requires a precision in the positioning of boundaries that is identical to, or better than, the manufacturing tolerances. If boundaries could only be

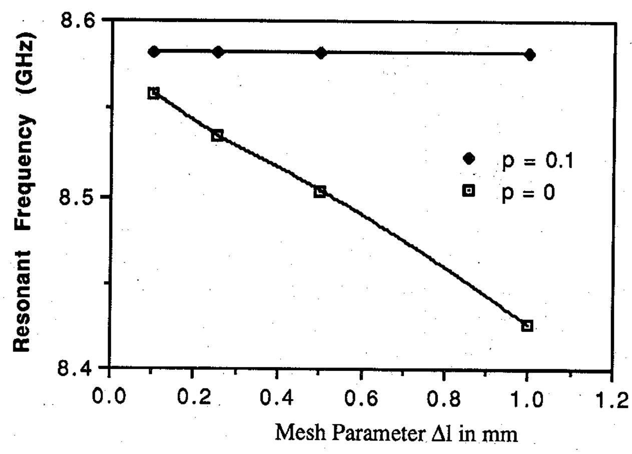

Fig. 8. Effect of the fifth branch of a corner node on the accuracy of TLM simulations of structures with sharp edges or corners.

introduced either across nodes or halfway between nodes, then the mesh parameter Δl would have to be very small indeed, leading to unacceptable computational requirements. Similar considerations apply when curved boundaries with relatively small radii of curvature must be modeled. It is therefore important to provide for arbitrary positioning of boundaries. The basis for this feature has been described already in 1973 by Johns [13] who, at the time, thought that the advantage of this procedure over stepped contour modeling was too small to warrant the additional complexity of the algorithm. However, this is not true when analyzing narrowband waveguide components such as filters. Furthermore, as mentioned in Section III-A, parallel implementation facilitates the inclusion of such features without penalty in computation speed.

Fig. 9 shows the concept of arbitrary wall positioning in two-dimensional TLM. The boundary branch which has a length different from $\Delta l/2$ is simply replaced by an equivalent branch of length $\Delta l/2$ having the same input admittance. This ensures synchronism, but requires a different characteristic admittance for the boundary branch and hence, a modification of the impulse scattering matrix of the boundary node (see [13]). The effect of such boundary tuning is shown in Fig. 10 which indicates that the length of the boundary branch can be continuously tuned over a range of more than one mesh parameter Δl without appreciable error. This important technique definitely removes the restriction that dimensions of TLM models can only be integer multiples of the mesh parameter.

An alternative technique which can easily be applied to the 3-D case as well consists of replacing the excess length of an irregular boundary branch beyond the $\Delta l/2$ position by an equivalent inductance or capacitance (which will be independent of frequency as long as $\Delta l/\lambda << 1$) and to discretize the differential equation governing the relation between voltage and current in this element [14]. This results in the following general recursive formula:

$$ {}_kV^i = \rho \frac{\kappa - 1}{\kappa + 1} {}_kV^r + \frac{\kappa}{\kappa + 1} (\rho_{k-1}V^r + {}_{k-1}V^i) \quad (1) $$

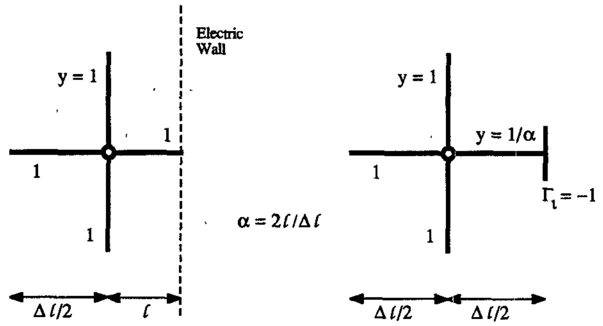

Fig. 9. Modification of boundary node for arbitrary position of boundary.

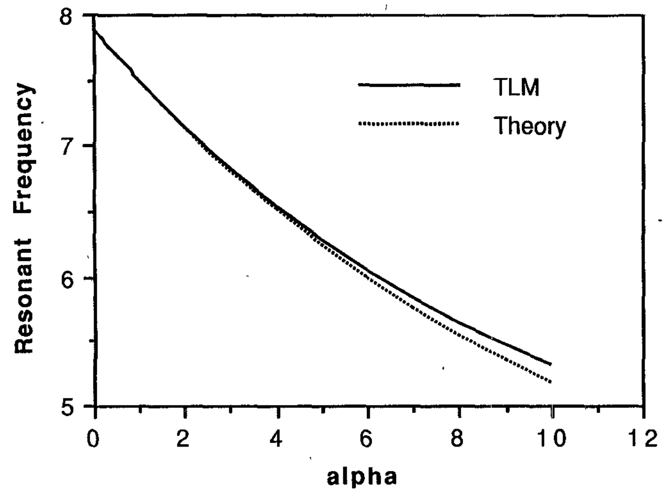

Fig. 10. Resonant frequency of a quarter-wave resonator terminated by a tunable electric wall as a function of the relative position $\alpha = 2l/\Delta l$.

where $\rho = +1$ for a magnetic wall and $\rho = -1$ for an electric wall. κ is equal to $2l/\Delta l$ in the 3-D TLM case, and $\sqrt{2l/\Delta l}$ in the 2D TLM case. Equation (1) indicates that the present impulse reflected from the boundary in the reference plane at $\Delta l/2$ depends on the present incident impulse as well as on the previous incident and reflected impulses, which need to be stored. This recursive algorithm amounts to a numerical procedure for integrating the differential equation describing the behavior of the reactive stub in the time domain.

These techniques effectively free the modeler from the restrictions of the "Manhattan-style" or staircase approximation of curved boundaries and provides the necessary flexibility for fine adjustments of structure dimensions without resorting to graded mesh techniques.

B. Implementation of Moving Boundaries

Since the position parameter $\alpha = 2l/\Delta l$, or the factor κ in (1), can be continuously varied during a simulation, this feature can be used to model moving boundaries. This means that the position of a boundary can be changed by an arbitrarily small amount between computational steps. This opens possibilities not available in frequency domain simulators, such as the modeling of expansion or contraction of objects during a simulation (temperature effects), the influence of wall vibrations on the electromagnetic behaviour of structures, Doppler effect, etc. It also allows the modeler to adjust or tune circuit dimensions during a simulation without the need for exciting the structure anew after every modification. This is because the field solution before the modification can be regarded as a slightly perturbed state of the field in the modified structure, and the transition between the two solutions is faster than the buildup of a new solution from the zero field state. It becomes thus feasible to tune, for example, a resonator in the time domain by exciting it only once, and when the field is built up, by moving (tuning) one or several of its walls and observing the change in its resonant frequencies. This tuning process may be combined with an optimization strategy, or be executed directly by the operator using visual feedback, thus realistically simulating the tweaking of the dimensions of a physical circuit.

V. Numerical Synthesis through Time Reversal

It has been shown recently by Sorrentino *et al.* [15] that the impulsive excitation of a linear lossless TLM network can be exactly reconstructed from the solution it produces, by inverting the TLM process. This is a direct consequence of the properties of the TLM impulse scattering matrix which is always equal to its inverse. In order to relate this fact to the numerical synthesis of microwave structures, consider a perfectly conducting body in space or in a waveguide. Finding the topology of such a scatterer amounts to reconstructing from the radiated fields the position of the current sources induced on its surface. In a forward simulation of a scattering process, the field function ϕ_{tot} in space is a superposition of the incident and the scattered fields:

$$\phi_{\text{tot}} = \phi_{\text{inc.}} + \phi_{\text{scatt}} \tag{2}$$

Hence, in order to obtain the field $\phi_{\text{scatt.}}$ due to the induced sources alone, the incident field $\phi_{\text{inc.}}$ (or homogeneous solution) must be computed separately and then subtracted at each node from the total solution ϕ_{tot}. From this difference, the induced source and hence, the topology of the scatterer, can then be reconstructed by inverse TLM simulation.

To demonstrate this process for a very simple case, consider the situation shown in Fig. 11. It shows two identical sections of parallel plate waveguide which are terminated at each end with wideband absorbing boundaries. The upper guide is empty, while the lower guide contains a discontinuity in the form of a thin, perfectly conducting septum. A Gaussian pulse is now injected from the left into both structures (Fig. 11(a)). It travels unchanged through the upper homogeneous section, but is scattered by the septum in the lower section (Fig. 11(b) and (c)). The output nodes situated at both extremities capture the response of the upper section (incident or homogeneous solution), and that of the lower section (total field solution), shown here after 30, 70, and 100 iterations (a, b, and c, respectively). The difference of the responses of the empty and the loaded section is then computed and

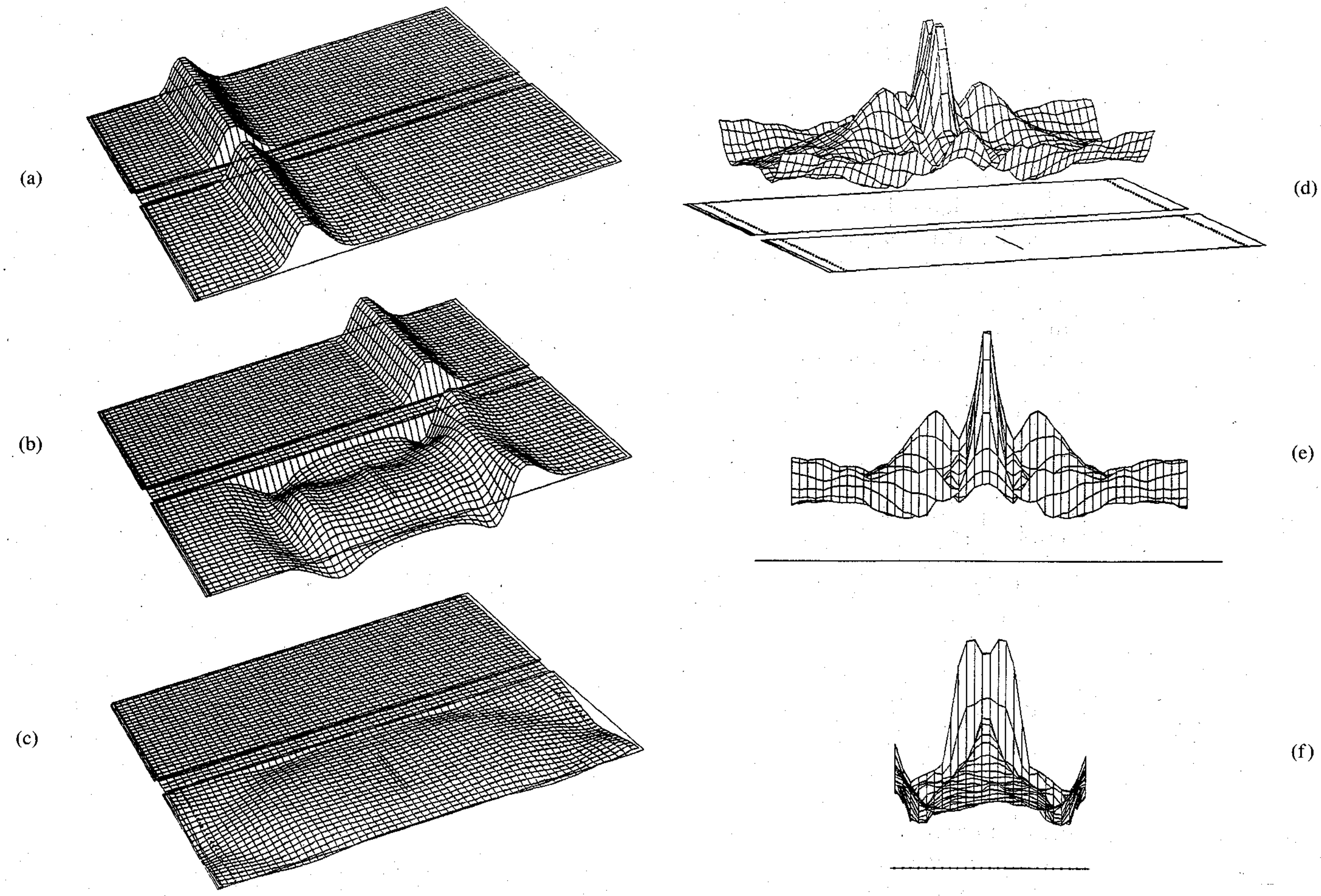

Fig. 11. Two identical matched parallel plate waveguide sections are shown. The upper section is empty, and the lower contains a conducting septum. (a) to (c) show the fields due to injection of a Gaussian pulse from the left after 30, 70, and 100 iterations. The difference betweern the two responses is re-injected into the empty section in reverse time sequence. (d) to (f) show the maximum field after re-injection, reconstructing the position of the septum within the rather coarse resolution of the pulse.

re-injected into the empty section through the same rows of nodes in reversed time sequence, and the maximum field value occurring at each node during the entire reverse simulation is recorded. Fig. 11(d) to (f) show the result of this inverse process in perspective, longitudinal and transversal view. It can be seen that this procedure yields the exact position of the septum as expected. Obviously, the spatial resolution of the reconstruction in the transverse dimension is inversely proportional to the spatial width of the exciting Gaussian pulse, which is rather coarse in this case, and directly proportional to the mesh parameter Δl. However, the exact dimensions can be extracted by further processing (see [16]).

In a practical CAD problem, however, the specifications are not available as a time domain response, but more likely as a frequency response over a restricted frequency range. This information is insufficient for the reconstruction of the circuit topology yielding this response, and the designer must therefore generate the missing information somehow. It will be shown below how this is done in the case of the septum in Fig. 11. (see also [16]). Obviously, this septum acts as a shunt inductance in the operating band of the dominant mode. It is well known that the frequency response of a shunt inductance can be produced by many types of obstacles other than a septum (posts of rectangular, elliptical or irregular cross-section, irises, etc.) in various lateral positions. Therefore, the designer must first select an appropriate type of obstacle based on other considerations, such as available technology or ease of manufacturing. Then, an obstacle with approximately the right dimensions can be selected as a starting guess using available formulas for the shunt susceptance in terms of the dimensions.

For this starting obstacle the impulse response is then generated with a forward TLM analysis. The dominant mode content of this first response $\Phi^{t}_{\text{left}}(i, k)$ and $\Phi^{t}_{\text{right}}(i, k)$ is extracted at both extremities of the waveguide section, Fourier transformed and replaced by the desired (specified) dominant mode content in the frequency domain. The modified total response is then transformed back into the time domain and, reduced by the homogeneous response of the empty waveguide, reinjected into the computational domain in the inverse time sequence. This procedure will now be described in more detail.

Let the impulse response of the approximate obstacle be $f_1(t)$ with its Fourier transform $F_1(\omega)$. The latter is most likely different from the desired (specified) frequency response $F_2(\omega)$ which is usually defined over a restricted frequency range and for the dominant mode only. We can thus modify $F_1(\omega)$ so that it is identical to $F_2(\omega)$ in the bandwidth of interest, and for the dominant mode or propagation. Now the modified response $F_1'(\omega)$ must be converted to a time domain signal for reinjection into the empty waveguide.

Since $F_1(\omega) - F_1'(\omega)$ is limited to the frequency band in which only the dominant mode can propagate, the transverse field distribution of the corresponding time function $f_1(t) - f_1'(t)$ is known. The time domain signal corresponding to the modified frequency response is thus

$$f_1'(t) = f_1(t) - \underbrace{\mathfrak{F}^{-1}[F_1(\omega) - F_2(\omega)]}_{\text{known transversal distribution}}. \tag{3}$$

This new time domain impulse response $f_1'(t)$ approximates the wanted impulse response since it contains, for the bandwidth of interest, the dominant mode response of the obstacle to be synthesized.

Finally, the difference between $f_1'(t)$ and the homogeneous response is injected into the empty structure in reversed time sequence, yielding an image of the synthesized obstacle as described above. This represents an improvement over the initial guess and in many cases, is already acceptable as a final result. However, if a new forward analysis still yields an unsatisfactory answer, the same sequence is repeated until the analysis satisfies specifications. In the case of single obstacles this process converges rather quickly, and typically two or three forward-and-backward simulation cycles yield the final geometry. Synthesis of larger circuit configurations is currently under study.

VI. User Interface and Typical Simulation Results

Since the user of a time domain electromagnetic simulator must enter every physical and electrical detail of a structure under test, the graphical interface must be very friendly and well conceived. It consists typically of a 3-D geometrical editor window which is similar to a 3-D drafting environment, a source window for specifying the excitation waveforms, an analyzer window for displaying time domain and frequency domain output as well as S-parameters, and an animator window for visualizing propagating fields. Figs. 12 to 15 show some typical examples (screen dumps) generated with a 3-D geometry-based TLM-Simulator prototype developed at the University of Ottawa.

Fig. 12 reproduces the geometrical editor window containing a microstrip meander line and a straight microstrip section side by side, shown from three co-ordinate directions and in perspective. The structures are enclosed by absorbing boundaries simulating open space. Fig. 13 visualizes the propagation of a Gaussian pulse through both the meander and reference lines. Obviously, this representation does not fully reproduce the effect of the dynamic display which shows the motion of the fields. (To give some idea of the time needed to run this simulation, each iteration requires about one second on a DEC 3100 RISC workstation. This includes the time for graphics. More powerful workstations with visualization hardware will require only a small fraction of a second for one iteration). Fig. 14 compares three time domain signals picked up at the extremities of the lines. They clearly show the effects of dispersion on the travelling waveform, the delay in the meander line, and the effects of surface wave

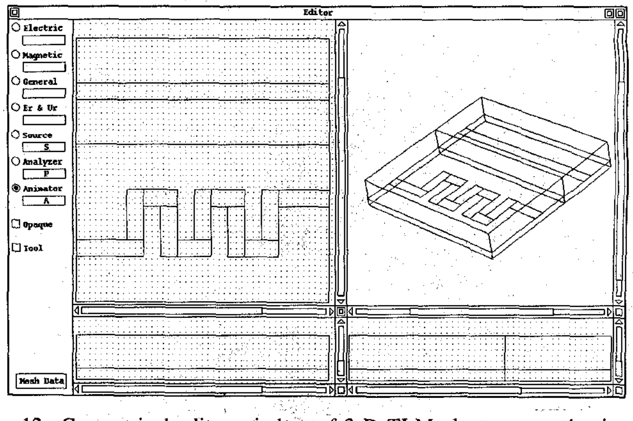

Fig. 12. Geometrical editor window of 3-D TLM electromagnetic simulator. It shows a microstrip meander line and a reference section in a box with absorbing top and side walls.

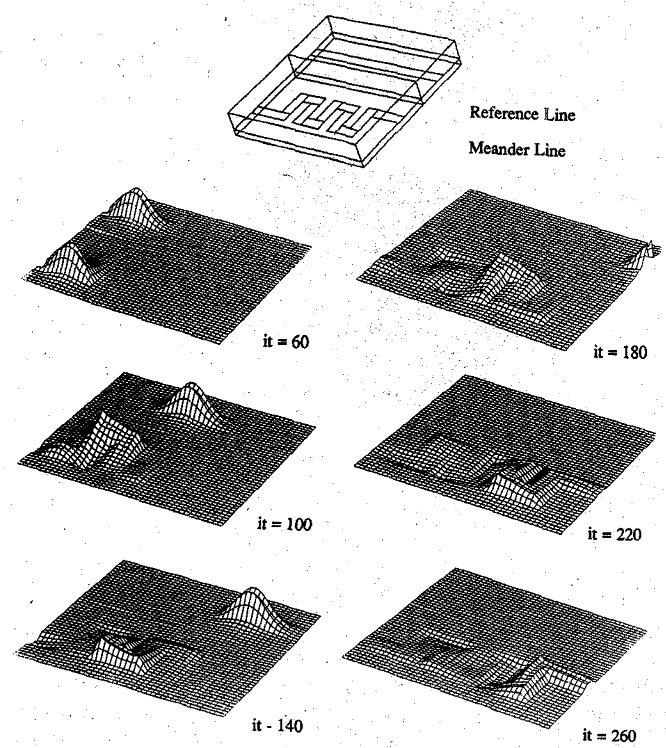

Fig. 13. Propagation of a Gaussian pulse through the meander line and the straight reference line.

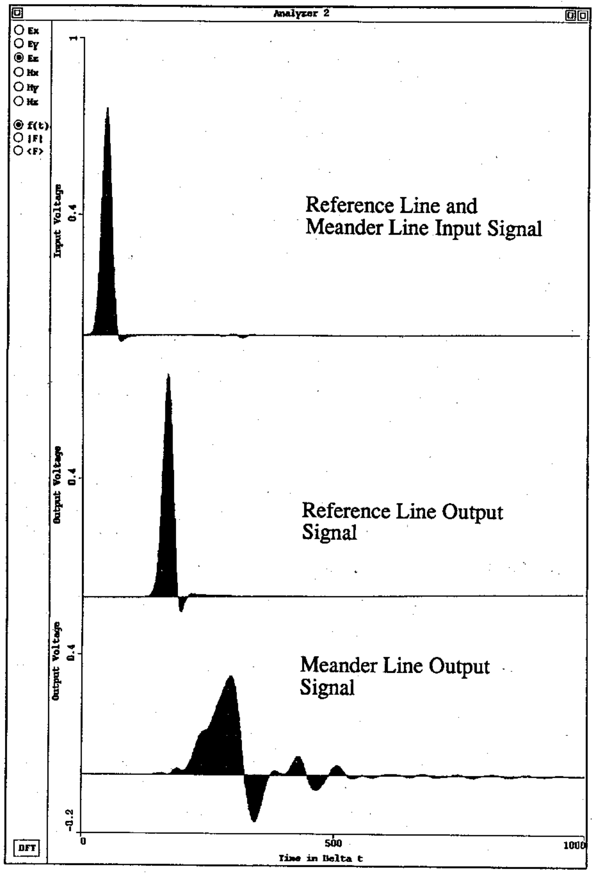

Fig. 14. Time domain signals at the input and output of the two lines.

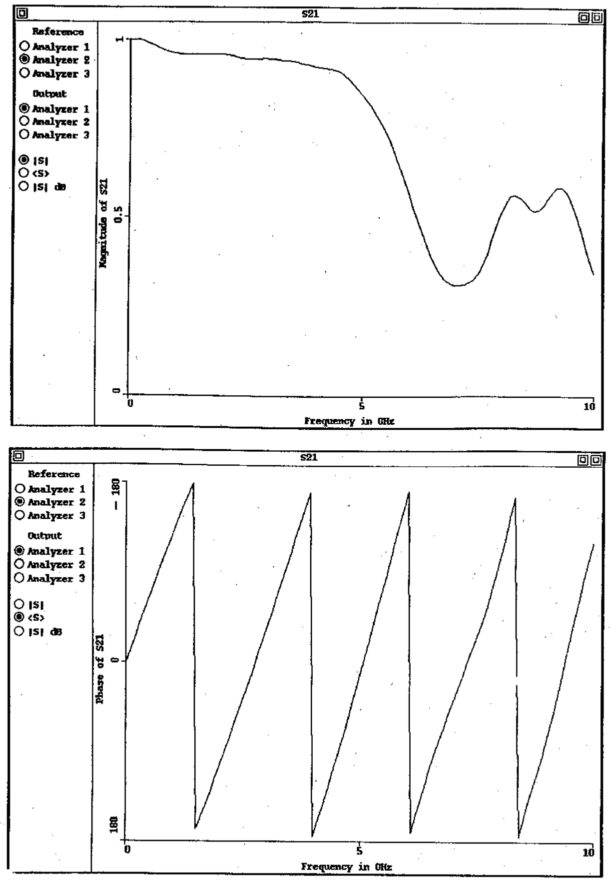

Fig. 15. Magnitude and phase of S_{21} extracted from the time domain signals in Fig. 14 by discrete Fourier transform.

propagation (precursor in the meander line output signal) and of multiple discontinuity reflections (tail of meander line output signal). Finally, Fig. 15 shows the ratio of the complex Fourier transforms of the time domain signals (meander output/reference input) yielding S_{21} in magnitude and phase.

The time domain simulator thus emulates the functions of a 3-D drafting machine, a video system, a time domain reflectometer, a network analyser and a spectrum analyzer, in other words a complete microwave laboratory in a single computer tool.

VII. Discussion and Conclusion

While most of the basic time domain modeling procedures have now been demonstrated and implemented in various computer programs, the considerable computer time and memory required to model realistic electromagnetic structures is still an obstacle when it comes to realizing professional CAD tools based on these techniques. Therefore, considerable research efforts are concentrating on measures to reduce the computation count to manageable levels. In this paper three different ways to achieve this have been described, namely parallel processing to accelerate the TLM process itself, Prony–Pisarenko signal processing to reduce the required number of computation steps, and coarseness error compensation at sharp corners and edges. All these methods can be combined to accelerate TLM simulations by several orders of magnitude. Since the computation count for TLM analyses increases faster than the fourth power of the linear mesh density, these accelerating features enhance our ability to model complex structures to a much greater extent than the mere increase of memory size and speed of computers. Procedures for fine tuning of wall positions have also been described. The ability to position boundaries at arbitrary distances from TLM mesh nodes not only provides higher modeling accuracy and resolution but also minimizes required computer resources. Since a time domain simulator explicitly stores all geometrical and electrical characteristics of a structure under test, it can directly be linked with manufacturing and processing facilities. Furthermore, it can produce time domain and frequency domain data in a format suitable for input into other CAD tools.

Future time domain CAD systems will most likely employ dedicated parallel processors configured in a 3-D array. Furthermore, the nature of discrete time domain algorithms gives rise to simulation procedures which differ considerably from those employed in traditional frequency domain CAD tools. These include the implementation of moving boundaries for geometrical tuning during a simulation as well as numerical synthesis through reversal of the TLM process in time. Considerable research is still required to bring all these procedures to full maturity, but it is conceivable that at the present rate of progress in time domain modeling, these techniques will equal, and in many aspects, surpass the capabilities of frequency domain CAD tools in the next decade.

References

[1] S. Akhtarzad and P. B. Johns, "Solution of Maxwell's equations in three space dimensions and time by the T.L.M. method of analysis," *Proc. Inst. Elec. Eng.*, vol. 122, no. 12, pp. 1344–1348, Dec. 1975.

[2] K. S. Yee, "Numerical solution of initial boundary value problems involving Maxwell's equations, in isotropic media," *IEEE Trans. Antennas Propagat.*, vol. AP-14, no. 5, pp. 302–307, May 1966.

[3] P. B. Johns, "A Symmetrical condensed node for the TLM method," *IEEE Trans. Microwave Theory Tech.*, vol. MTT-35, no. 4, pp. 370–377, Apr. 1987.

[4] Z. Chen, W. J. R. Hoefer, and M. Ney, "A new finite-difference time-domain formulation and its equivalence with the TLM symmetrical condensed Node," *IEEE Trans. Microwave Theory Tech.*, vol. 39, no. 12, pp. 2160–2169, Dec. 1991.

[5] J. Nielsen and W. J. R. Hoefer, "A complete dispersion analysis of the condensed node TLM mesh," in *4th Biennial IEEE Conf. Electromagnetic Field Computation Dig.*, Toronto, ON., Oct. 22–24, 1990.

[6] P. P. M. So and W. J. R. Hoefer, "3D-TLM time domain electromagnetic wave simulator for microwave circuit modeling," in *1991 IEEE MTT-S Int. Microwave Symp. Dig.*, Boston, June 11–13, 1991, pp. 631–634.

[7] P. P. M. So, Eswarappa, and W. J. R. Hoefer, "A two-dimensional TLM microwave field simulator using new concepts and procedures," *IEEE Trans. Microwave Theory Tech.*, vol. 37, no. 12, pp. 1877–1884, Dec. 1989.

[8] M. A. Morgan, Ed., "Finite element and finite difference methods in electromagnetic scattering," in *PIER 2 Progress in Electromagnetics Research*, New York: Elsevier, 1990.

[9] C. T. Tong and Y. Fujino, "An efficient algorithm for transmission line matrix analysis of electromagnetic problems using the symmetrical condensed node," *IEEE Trans. Microwave Theory Tech.*, vol. 39, no. 8, pp. 1420–1424, Aug. 1991.

[10] J. L. Dubard, D. Pompei, J. Le Roux, and A. Papiernik, "Characterization of microstrip antennas using the TLM simulation associated with a Prony–Pisarenko method," *Int. J. Numerical Modelling*, vol. 3, no. 4, pp. 269–285, Dec. 1990.

[11] W. L. Ko and R. Mittra, "A combination of FD-TD and Prony's method for analyzing microwave integrated circuits," *IEEE Trans. Microwave Theory Tech.*, vol. 39, no. 12, pp. 2176–2181, Dec. 1991.

[12] U. Müller, P. P. M. So, and W. J. R. Hoefer, "The Compensation of Coarseness Error in 2D TLM Modeling of Microwave Structures," in *1992 IEEE MTT-S Int. Microwave Symp. Dig.*, Albuquerque, NM, June 1–5, 1992.

[13] P. B. Johns, "Transient analysis of waveguides with curved boundaries," *Electron. Lett.*, vol. 9, no. 21, Oct. 18, 1973.

[14] U. Müller, A. Beyer, and W. J. R. Hoefer, "The implementation of smoothly moving boundaries in 2D and 3D TLM simulations," in *1922 IEEE MTT-S Int. Microwave Symp. Dig.*, Albuquerque, NM, June 1–5, 1992.

[15] R. Sorrentino, P. P. M. So, and W. J. R. Hoefer, "Numerical microwave synthesis by inversion of the TLM Process," in *21st European Microwave Conf. Dig.*, Stuttgart, Germany, Sept. 9–12, 1991.

[16] M. Forest and W. J. R. Hoefer, "TLM synthesis of microwave structures using time reversal," in *1992 IEEE MTT-S Int. Microwave Symp. Dig.*, Albuquerque, NM, June 1–5, 1992.

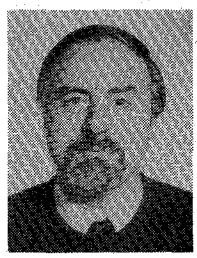

Wolfgang J. R. Hoefer (M'71–SM'78–F'91) received the Dipl.-Ing. degree in Electrical Engineering from the Technische Hochschule Aachen, Germany, in 1965, and the D. Ing. degree from the University of Grenoble, France, in 1968.

During the academic year 1968–1969 he was a Lecturer at the Institut Universitaire de Technologie de Grenoble and a Research Fellow at the Institut National Polytechnique de Grenoble, France. In 1969 he joined the Department of Electrical Engineering, the University of Ottawa, Canada where he was a Professor until March 1992. He presently holds the NSERC/MPR Teltech Industrial Research Chair in RF Engineering in the Department of Electrical and Computer Engineering, the University of Victoria, Canada. During sabbatical leaves he spent six months with the Space Division of AEG-Telefunken in Backnang, Germany (now ATN), and six months with the Electromagnetics Laboratory of the Institut National Polytechnique de Grenoble, France, in 1976–1977. During 1984–1985 he has been a visiting scientist at the Space Electronics Directorate of the Communications Research Centre in Ottawa, Canada. He spent a third sabbatical year in 1990–1991 as a visiting professor at the University of Rome "Tor Vergata" in Italy, the University of Nice-Sophia Antipolis in France, and the Technical University of Munich in Germany.

His research interests include numerical techniques for modeling electromagnetic fields and waves, computer aided design of microwave and millimeter wave circuits, microwave measurement techniques, and engineering education. Professor Hoefer is a Registered Professional Engineer.